Vol. 22: 99–113, 2002 | CLIMATE RESEARCH Clim Res | Published September 6

A knowledge-based approach to the statistical mapping of climate

Christopher Daly[1,*], Wayne P. Gibson[1], George H. Taylor[1], Gregory L. Johnson[2], Phillip Pasteris[2]

[1]Spatial Climate Analysis Service, Department of Geosciences, and College of Oceanographic and Atmospheric Sciences, 316 Strand Agricultural Hall, Oregon State University, Corvallis, Oregon 97331-2209, USA,

[2]USDA-NRCS National Water and Climate Center, 101 SW Main, Suite 1600, Portland, Oregon 97204-3224, USA

ABSTRACT: The demand for spatial climate data in digital form has risen dramatically in recent years. In response to this need, a variety of statistical techniques have been used to facilitate the production of GIS-compatible climate maps. However, observational data are often too sparse and unrepresentative to directly support the creation of high-quality climate maps and data sets that truly represent the current state of knowledge. An effective approach is to use the wealth of expert knowledge on the spatial patterns of climate and their relationships with geographic features, termed 'geospatial climatology', to help enhance, control, and parameterize a statistical technique. Described here is a dynamic knowledge-based framework that allows for the effective accumulation, application, and refinement of climatic knowledge, as expressed in a statistical regression model known as PRISM (parameter-elevation regressions on independent slopes model). The ultimate goal is to develop an expert system capable of reproducing the process a knowledgeable climatologist would use to create high-quality climate maps, with the added benefits of consistency and repeatability. However, knowledge must first be accumulated and evaluated through an ongoing process of model application; development of knowledge prototypes, parameters and parameter settings; testing; evaluation; and modification. This paper describes the current state of a knowledge-based framework for climate mapping and presents specific algorithms from PRISM to demonstrate how this framework is applied and refined to accommodate difficult climate mapping situations. A weighted climate-elevation regression function acknowledges the dominant influence of elevation on climate. Climate stations are assigned weights that account for other climatically important factors besides elevation. Aspect and topographic exposure, which affect climate at a variety of scales, from hill slope to windward and leeward sides of mountain ranges, are simulated by dividing the terrain into topographic facets. A coastal proximity measure is used to account for sharp climatic gradients near coastlines. A 2-layer model structure divides the atmosphere into a lower boundary layer and an upper free atmosphere layer, allowing the simulation of temperature inversions, as well as mid-slope precipitation maxima. The effectiveness of various terrain configurations at producing orographic precipitation enhancement is also estimated. Climate mapping examples are presented.

KEY WORDS: Climate map · Knowledge-based system · Climate interpolation · Spatial climate · Climate data sets · GIS · PRISM · Geospatial climatology

1. INTRODUCTION

The demand for spatial climate data sets in digital form has risen dramatically in recent years, as computer technology has enabled a variety of hydrologic, ecological, natural resource, and other models and decision systems to be linked to geographic information systems (GIS) (Nemani et al. 1993, Neilson 1995, Nusser & Goebel 1997). Methods for mapping climate from point data fall into 2 main categories: human-

*E-mail: daly@coas.oregonstate.edu

expert and statistical. Human-expert methods use human experience, expertise, and knowledge acquisition capabilities to infer climate patterns from meteorological regimes, physiographic features, biotic characteristics, and other information sources. They involve the manual preparation of climate maps (Reed & Kincer 1917, Peck & Brown 1962), often based on topographic analyses involving the correlation of point climate data with an array of topographic and synoptic parameters such as topographic position, slope, exposure, elevation, location of barriers, and wind speed and direction (Spreen 1947, Burns 1953, Stoeckeler 1963, Schermerhorn 1967, Hovecar & Martsolf 1971, Bootsma 1976, Houghton 1979, Basist et al. 1994). Most of the 'official' precipitation maps for US states were created in the 1960s by federal agencies using human-expert methods. These maps were widely accepted as reflecting the best understanding of spatial climate distribution at the time.

Statistical procedures use a numerical function, calculated or prescribed, to weight irregularly spaced point data to estimate a regularly spaced prediction grid. Inverse-distance weighting is an example of a simple statistical interpolation method. Adaptations of this concept have been used for climate interpolation (Shepard 1968, Renka 1984, Willmott et al. 1985, Dodson & Marks 1997, Thornton et al. 1997). Kriging and its variants (Matheron 1971) have been applied extensively to the interpolation of climate data (Dingman et al. 1988, Hevesi et al. 1992, Phillips et al. 1992, Garen et al. 1994). Kriging involves the development of 1 or more semivariogram models that best fit the data to arrive at optimum station weights for interpolation. Splining is a related statistical method useful in climate interpolation (Wahba & Wendelberger 1980, Hutchinson 1995).

Maps created by objective statistical methods rarely provide the accuracy, detail, and realism required to supersede manually drawn maps as the official versions. Hence, few of the official maps produced in the 1960s have been updated with statistically generated maps. While computerized statistical approaches have a great potential advantage over human-expert methods in terms of speed, consistency, and repeatability, they lack a spatial climate knowledge base that can be drawn upon to fill the need for expertise and experience in the mapping process.

A well-known discipline in computer science known as knowledge-based system (KBS) technology provides a useful framework for an effective way to combine the strengths of both human-expert and statistical methods. Climate mapping situations are ideal candidates for the application of a KBS approach; data are unrepresentative and new and unexpected situations continually arise, but a large body of expert knowledge is available. KBS technology is a companion to expert systems, one of the most successful branches of artificial intelligence research (Doukidis & Whitley 1988, Studer et al. 1999). KBS has been applied in the fields of computer science, natural resource management (Schmoldt & Rauscher 1996), hydrologic modeling (Lam & Swayne 1993), meteorology (Jones & Roydhouse 1994), and GIS (geographical information systems; Yuan 1997). Applications of KBS to spatial problems in GIS are a particularly useful analogue for climate mapping, because both involve spatial problems, which are inherently difficult to solve using generalized computational techniques. KBS holds promise as a method by which new functions can be developed and added to the range of specialized methods available for analyzing spatial data (Holt & Benwell 1999).

An example of a combined statistical/human-expert approach to climate mapping using KBS is PRISM (parameter-elevation regressions on independent slopes model) (Daly & Neilson 1992, Daly et al. 1994, 1997, 2001, Johnson et al. 2000). PRISM is a regression-based model that uses point data, a digital elevation model (DEM), other spatial data sets, a knowledge base, and human-expert parameterization to generate repeatable estimates of annual, monthly and event-based climatic elements. These estimates are interpolated to a regular grid, making them GIS-compatible.

The quality of the PRISM climate maps has been sufficient to enable large-scale updates of the official climate maps produced in the 1960s by human-expert methods. Recent PRISM mapping work includes the first official updates of manually-drawn USDA precipitation and temperature maps for all 50 states (e.g. USDA-SCS 1965), peer-reviewed by about 40 experts (Bishop et al. 1998, USDA-NRCS 1998, Daly & Johnson 1999, Vogel et al. 1999, Daly et al. 2001); the first official update of the manually drawn Climate Atlas of the United States (USDOC 1968), reviewed and approved by the National Climatic Data Center (Plantico et al. 2000); a high-resolution, 103 yr series of monthly temperature and precipitation maps for the conterminous 48 states (Daly et al. 1999, 2000b, 2001); detailed precipitation and temperature maps for Canada (e.g. Environment Canada 2001), China and Mongolia (Daly et al. 2000a); and the first comprehensive precipitation maps for the European Alps region, produced for the Hydrologic Atlas of Switzerland (Schwarb et al. 2001a,b).

The objective of this paper is to describe the thinking and rationale behind the development of a spatial climate KBS, and present working examples in the form of algorithms from PRISM. The paper begins with an overview of the spatial climate KBS (Section 2); followed by descriptions of associated algorithms, including the governing climate-elevation regression function (Section 3), the station weighting approach (Section 4), topographic facets (Section 5), coastal proximity (Section 6),

and the 2-layer atmosphere (Section 7). The paper ends with a summary and conclusions (Section 8).

2. A KNOWLEDGE-BASED SYSTEM FOR SPATIAL CLIMATE

The main components of a KBS are: (1) knowledge acquisition modules that elicit expert information; (2) a knowledge base in which the knowledge is stored; (3) an inference engine for inferring solutions to problems from stored knowledge; and (4) a user interface that allows the model to accept user input and explain its processing and reasoning steps (Forsyth 1989). We would add that an independent verification component is critical to the ongoing process of knowledge acquisition and refinement. Below are a presentation of the conceptual structure of the KBS for spatial climate and an overview of the knowledge base.

2.1. Conceptual structure of the KBS

Fig. 1 outlines the conceptual structure of a spatial climate KBS, using PRISM as an example of the central computer model. Our KBS is not a mature one, and the problem domain is very large. Therefore, knowledge must be accumulated, generalized, and refined through an ongoing process of model application; development of algorithm prototypes, parameters, and parameter settings; and verification of results. Over time, there is a slow but steady transfer of knowledge from the user to the model (thick arrow in Fig. 1).

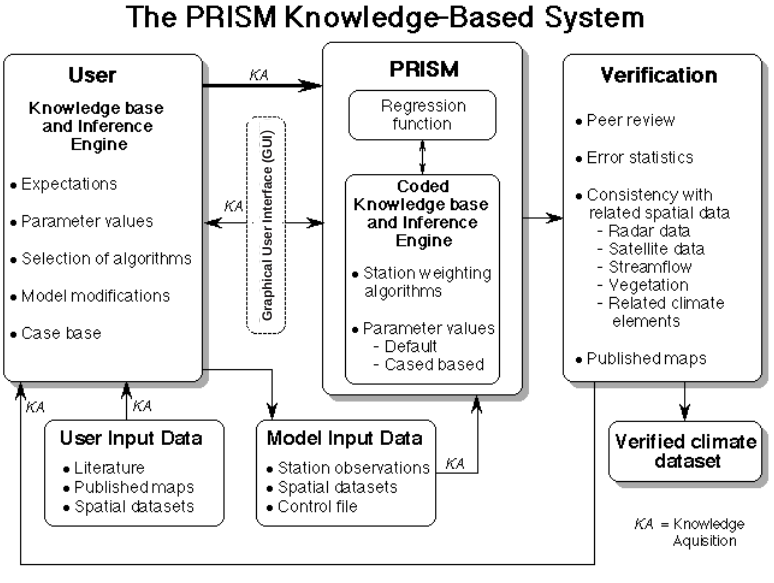

Fig. 1. The conceptual structure of a knowledge-based system for climate. The system contains 2 main centers of knowledge and inference: the user and the model. The user interacts with the model through a graphical user interface. Verification represents an independent source of knowledge. Knowledge is accumulated, generalized, and refined through an ongoing process of model application; development of algorithm prototypes, parameters, and parameter settings; and verification of results. Over time, there is a slow but steady transfer of knowledge from the user to the model (thick arrow)

The PRISM module consists of a local moving-window, climate-elevation regression function that interacts with an encoded knowledge base and inference engine. This knowledge base/inference engine is a series of rules, decisions and calculations that set weights for the station data points entering the regression function. In general, a weighting function contains knowledge about an important relationship between the climate field and a geographic or meteorological factor. The inference engine sets values for input parameters by using default values, or it may use the regression function to infer grid cell-specific parameter settings for the situation at hand. PRISM acquires domain knowledge through assimilation of station data; spatial data sets such as a terrain and others; and a control file containing parameter settings.

The other center of knowledge and inference is that of the user. The user accesses literature, previously published maps, spatial data sets, and a graphical user interface to guide the model application. One of most important roles of the user is to form expectations for the modeled climatic patterns, i.e. what is deemed 'correct'. Based on knowledgeable expectations, the user selects the station weighting algorithms to be used and determines whether any parameters should be changed from their default values. Through the graphical user interface, the user can click on any grid cell, run the model with a given set of algorithms and parameter settings, view the results graphically, and access a traceback of the decisions and calculations leading to the model prediction.

If the modeling system is to gain expertise over time, results must be subjected to a rigorous verification process that is as independent from the modeling system as possible. Model diagnostic statistics such as cross-validation error, confidence interval, and estimation variance give objective, quantitative feedback on performance, and they are useful in parameterizing the model for optimal numerical performance. However, these measures are highly dependent on model assumptions and completeness of the station data. Model results may be independently evaluated by assessing their consistency with other spatial elements, such as stream flow, vegetation

patterns, and related climate elements. Because the goal is to produce maps that best represent the state of (human) knowledge, the most useful source of verification may be that of domain experts who can give definite, justifiable feedback on how well the model results reproduce their best knowledge. This feedback can be in the form of evaluation of the spatial patterns and magnitudes of the mapped climate values, as well as insight into station data quality issues (Daly & Johnson 1999).

2.2. The knowledge base

The knowledge base encoded into PRISM contains key concepts that describe the spatial patterns of climate. The knowledge base draws upon over a century of observations and research in a discipline that can be termed 'geospatial climatology', the study of the spatial patterns of climate and their relationships with geographic features. The key concepts included to date are discussed briefly below.

2.2.1. Elevational influence on climate

Climate varies strongly with elevation. Temperature typically decreases with altitude, and precipitation generally increases (Oke 1978, Barry & Chorley 1987). Elevation is an excellent statistical predictor variable, because it is usually sampled at a far greater spatial density than climate variables and is often estimated on a regular grid (i.e. DEM). The PRISM moving-window climate-elevation regression function is discussed in Sections 3 and 4.

2.2.2. Terrain-induced climate transitions

In complex terrain, climatic patterns are defined and delineated by topographic slopes and barriers, creating a mosaic of hill slopes, or 'facets', each potentially experiencing a different climatic regime (Daly et al. 1994, Gibson et al. 1997). Topographic facets can be delineated at a variety of scales. The major leeward and windward sides of large mountain ranges occur at relatively large scales, while north- and south-facing hill slopes with different radiation regimes exist at small scales. PRISM topographic facet algorithms are discussed in Section 5.

2.2.3. Coastal effects

Proximity to a large water body can be a major determinant of climate regime. For example, gradients in summer maximum temperature can exceed 20°C in 5 to 20 km, and precipitation patterns are often delineated by proximity to coastal moisture sources. PRISM coastal proximity algorithms are discussed in Section 6.

2.2.4. Two-layer atmosphere

While climate usually varies with elevation monotonically, some cases arise for which a monotonic change is not realistic. Examples are mid-slope precipitation maxima where the moist boundary layer is shallow relative to the terrain height (Giambelluca & Nullet 1991, Juvik et al. 1993); and wintertime temperature inversions in sheltered valleys, where temperature increases of 2.5 to 3.0°C per 100 m are not uncommon. PRISM divides the atmosphere into 2 vertical layers to handle these situations (discussed in Section 7).

2.2.5. Orographic effectiveness of terrain

Terrain features produce varying precipitation-elevation gradients, depending partly on their effectiveness in blocking and uplifting moisture-bearing air. Steep, bulky features oriented normal to the flow can generally be expected to produce steeper precipitation-elevation slopes than low, gently rising, features oriented parallel to the flow. A discussion of how PRISM recognizes and accounts for differences in orographic effectiveness is not presented here due to space limitations, but is available from Daly (2002).

3. GOVERNING EQUATION — THE ELEVATION REGRESSION FUNCTION

PRISM encodes the assumption that for a localized region, elevation is the most important factor in the distribution of many climate elements, such as temperature and precipitation. A regression function between climate and elevation serves as the main predictive equation in the model. A linear regression was chosen over nonlinear functions such as polynomial regression and curve-fitting functions such as splining, because: (1) altitudinal variations of climate are often linear (Vuglinski 1972, Hibbert 1979, Hanson et al. 1982, Osborn 1984), or can be transformed to approximate linearity; (2) the linear function can be extrapolated in a stable fashion far beyond the elevational range of the data; and (3) the linear function can be easily manipulated to compensate for

inadequacies in the data, which are rarely sufficient to fully represent the vertical distribution of the climate element. A simple, rather than multiple, regression model was chosen because it is difficult to construct a knowledge base to account for and interpret the complex relationships between multiple independent variables and climate. For the time being, the knowledge base and inference engine concentrate on controlling for the effects of variables other than elevation by weighting the data points based on several factors, as will be discussed later.

The simple linear regression has the form:

$$Y = \beta_1 X + \beta_0;\ \beta_{1m} \le \beta_1 \le \beta_{1x} \quad (1)$$

where Y is the predicted climate element, β_1 and β_0 are the regression slope and intercept, respectively, X is the DEM elevation at the target grid cell, and β_{1m} and β_{1x} are the minimum and maximum allowable regression slopes (Table 1). The climate-elevation regression is developed from x,y pairs of elevation and climate observations supplied by station data. All stations

Table 1. Descriptions and typical ranges and default values of relevant PRISM parameters for regional-scale climatological modeling. In an application, the model operator may: (1) use the default values; (2) adjust the parameters based on expert judgement; or in some cases, (3) allow the model to estimate the values (see parameters annotated with [a] or [c]). Parameters showing only 1 (default) value are those that are infrequently varied from application to application

Name	Description	Typical min.default/max. values	
Regression function			
r	Radius of influence	30/50/100 km[a]	
s_f	Minimum number of on-facet stations desired in regression	3/5/8 stations[a]	
s_t	Minimum number of total stations desired in regression	10/15/30 stations[a]	
		Precipitation (km^{-1})[b]	**Temperature** (°C km^{-1})
β_{1m}	Minimum valid regression slope	Layer 1 0.0	−10
		Layer 2 −0.5	−10
β_{1x}	Maximum valid regression slope	Layer 1 3.0	0/10/20
		Layer 2 0.0	0
β_{1d}	Default valid regression slope	Layer 1 0.8	−6
		Layer 2 −0.2	−6
Distance weighting			
a	Distance weighting exponent	2.0	
F_d	Importance factor for distance weighting	0.8	
Elevation weighting			
b	Elevation weighting exponent	1.0	
F_z	Importance factor for elevation weighting	0.2	
Δz_m	Minimum station-grid cell elevation difference below which elevation weighting is maximum	100/200/300 m	
Δz_x	Maximum station-grid cell elevation difference above which elevation weight is zero	500/1500/2500 m	
Facet weighting			
c	Facet weighting exponent	0.0/1.5/2.0	
g_m	Minimum inter-cell elevation gradient, below which a cell is flat	1 m/cell[c]	
λ_x	Maximum DEM filtering wavelength for topographic facet determination	60/80/100 km	
Coastal proximity weighting			
p_x	Maximum coastal proximity difference, above which proximity weight is zero	Varies with application	
v	Coastal proximity weighting exponent	0.0/1.0/1.0	
Vertical layer weighting			
y	Vertical layer weighting exponent	0.0/1.0/1.0[c]	

[a]Can be optimized automatically with cross-validation statistics
[b]Precipitation-elevation slopes are normalized by the mean precipitation in the regression function, e.g. (100 mm km^{-1} slope)/(1000 mm mean precipitation) = 0.1 km^{-1} normalized slope
[c]Can be varied dynamically by the model

located within a user-specified maximum radius from the target grid cell (r) are entered into the regression function (Table 1). If necessary, the model expands the radius until the number of stations retrieved is greater than or equal to s_t, the minimum number of stations desired in each regression (Table 1). s_t is typically set to a value which represents a compromise between statistical robustness and a desire for local detail in the predictions; 10 to 30 stations is a common range.

It is necessary to place bounds on the regression slope, because sparse station data may not represent the local climate-elevation relationship accurately, especially if only a narrow range of elevations is available. If, during the regression calculations, β_1 initially falls outside of the range defined by β_{1m} and β_{1x}, β_1 is deemed invalid and attempts are made to correct the problem by omitting stations one by one and rerunning the regression, starting with those with the lowest weights (station weighting is discussed below) and proceeding to those with greater weights. The omission process ends when either β_1 falls within the valid range or the total number of stations falls to s_t. If β_1 remains invalid when s_t is reached, β_1 is assigned the value of β_{1d}, the default slope for that layer. β_{1d} is usually set to the mean regression slope for the modeling domain (Table 1).

β_{1d}, β_{1m} and β_{1x} can be set separately for the 2 atmospheric layers described in Section 7. For precipitation, they are expressed in units that are normalized by the average observed value of the climate element in the regression data set for the target cell. Evidence gathered during model development indicates that this method of expression is relatively stable in both space and time (Daly et al. 1994).

Values of r, s_t, and s_f (s_f is the number of stations desired on the same topographic facet; see Section 5 for discussion) can be determined through jackknife cross-validation (Daly et al. 1994). The combination of values that produces the lowest mean absolute prediction error (MAE) can be automatically adopted, or the user can elect to use other values for any of these parameters.

4. STATION WEIGHTING

Upon entering the regression function, each station is assigned a weight that is based on several factors. The combined weight, W, of a station is given as follows:

$$W = [F_d W(d)^2 + F_z W(z)^2]^{1/2}\ W(c)\,W(l)\,W(f)\,W(p)\,W(e) \quad (2)$$

where $W(d)$, $W(z)$, $W(c)$, $W(l)$, $W(f)$, $W(p)$, and $W(e)$ are the distance, elevation, cluster, vertical layer, topographic facet, coastal proximity, and effective terrain weights, respectively. F_d and F_z are the distance and elevation weighting importance factors. All weights and importance factors, individually and combined, are normalized to sum to unity. Distance and elevation weighting are discussed in this section, facet weighting in Section 5, coastal proximity weighting in Section 6, vertical layer weighting in Section 7, and effective terrain height in Daly (2002). Cluster weighting, not discussed in detail here, seeks to down-weight stations that are located in tight clusters to minimize over-representation of one particular location over others in the regression function.

The distance and elevation weighting importance factors, F_d and F_z, apply a measure of scaling to the vertical dimension by controlling the relative importance of distance and elevation in the regression equation. In model applications, the influence of horizontal distance on inter-station correlation seems to be greater overall than that of vertical distance. Thus, F_d is typically set to 0.8 and F_z to 0.2 (Table 1).

A station's influence in the regression function is assumed to decrease as its distance from the target grid cell increases. The distance weight is given as:

$$W(d) = \begin{cases} 1; & d = 0 \\ \dfrac{1}{d^a}; & d > 0 \end{cases} \quad (3)$$

where d is the horizontal distance between the station and the target grid cell and a is the distance weighting exponent. a is typically set to 2, which is equivalent to an inverse-distance-squared weighting function (Table 1).

Elevation weighting allows the model to focus on a vertical range that is specific to the target grid cell, thereby accommodating climate profiles that may vary in slope across the altitudinal range of the data. A station's influence in the regression function is assumed to decrease as its vertical, or elevational, distance from the target grid cell increases. Elevation weight is calculated as follows:

$$W(z) = \begin{cases} \dfrac{1}{\Delta z_m^b}; & \Delta z \le \Delta z_m \\ \dfrac{1}{\Delta z^b}; & \Delta z_m < \Delta z < \Delta z_x \\ 0; & \Delta z \ge \Delta z_x \end{cases} \quad (4)$$

Δz is the absolute elevation difference between the station and the target grid cell, b is the elevation weighting exponent, Δz_m is the minimum elevation difference, and Δz_x is the maximum elevation difference. b, Δz_m, and Δz_x are parameters (Table 1). b is typically set

to 1.0, which is equivalent to a 1-dimensional inverse-distance weighting function. Δz_m is the elevation difference below which the elevation weight is 1. Use of Δz_m creates a 'plateau', whereby stations just a few 10s of vertical meters from the target grid cell elevation do not dominate the regression to the exclusion of others, perhaps only 100 vertical meters away. A typical Δz_m varies from about 100 to 300 m. Δz_x is the elevation difference beyond which elevation weighting is zero. This enables data point inclusion to be restricted to a local elevation range. A typical Δz_x ranges from 500 to 2500 m (Table 1).

5. TOPOGRAPHIC FACETS

A topographic facet is a contiguous terrain slope with a common orientation, delineated at a variety of scales, from the major leeward and windward sides of large mountain ranges to north- and south-facing hill slopes. At each grid cell, the model chooses the topographic facet scale that best matches the data density and terrain complexity, and assigns the highest weights to stations on the same topographic facet. The model can also be configured to estimate the climatic significance of the facets, reducing the weighting exponent when facets appear to have little climatological importance.

5.1. Delineation of topographic facets

Effective delineation of facet orientation is not a straightforward process. Tests using simple vector averages of the east-west and north-south components of elevation gradients produced misleading results, especially along ridge lines and valley bottoms, where the directional gradient was not easily identified. The current method for delineating topographic facets is described in Gibson et al. (1997) and is summarized here.

Facet grids are constructed for 6 DEM smoothing levels, or scales (Daly et al. 1994). The smoothed DEM for each level is prepared by applying a modified Gaussian filter (Barnes 1964) to the original DEM. The filtering wavelength for each of the 6 levels is controlled by a user-defined maximum wavelength (λ_x) (Table 1). The DEM is filtered at equal intervals between a wavelength equal to the DEM resolution and λ_x. The orientation of each cell is computed from elevation gradients between the 4 adjacent cells (Daly et al. 1994) and assigned to an orientation bin on an 8-point compass. Elevation gradients less than a user-defined constant (g_m) are considered flat (Table 1). At higher wavelengths, a distribution of orientation bins is created for the target cell by calculating the orientations of all neighboring cells within a radius that matches the filter wavelength. The frequency distribution of bins is simplified using a set of 15 rules, as described in Gibson et al. (1997). The rule that best matches the distribution is used to assign an orientation to the target grid cell.

Operationally, a combination of station data density and local terrain complexity determines the appropriate facet smoothing level for a target grid cell. To find this level, PRISM attempts to retrieve a user-specified number of stations (s_f) that are on the same contiguous facet as the target cell. Starting with the smallest-wavelength facets at level 1, then proceeding to level 2 and beyond if necessary, PRISM accumulates stations until either s_f is reached or all facet levels have been exhausted.

5.2. Calculation of the facet weight

The facet weight for a station is calculated as:

$$W(f) = \begin{cases} 1; \ \Delta f \le 1 \text{ and } B = 0 \\ \dfrac{1}{(\Delta f + B)^c}; \Delta f > 1 \text{ or } B > 0 \end{cases} \quad (5)$$

where Δf is the absolute orientation difference between the station and the target grid cell (maximum possible difference is 4 compass points, or 180°), B is the number of intervening barrier cells with an orientation significantly different than that of the target grid cell, and c is the facet weighting exponent. A station is considered to be on the same facet as the target grid cell, and hence receives full facet weight, if it meets 2 conditions: (1) it resides on a cell that has a terrain orientation within one compass point of the target cell; and (2) the station's cell is located within the same group of similarly-oriented cells, or facet, as the target cell. The value of Δf quantifies condition 1, and B quantifies condition 2. B is calculated by identifying a line of cells that follows the shortest distance between a station and the target grid cell, and counting the total number of cells that do not possess orientations within one compass point of that of the target grid cell ($\Delta f > 1$). A value of B greater than zero indicates that there are grid cells with significantly different orientations between the station and the target cell, suggesting that the station is on a different facet. This helps discern between stations that are on the same contiguous facet as the target cell (i.e. the same mountain slope, where, $\Delta f = 1$ and $B = 0$) and those that happen to have the same orientation as the target cell, but reside on a completely different group of sim-

ilarly-oriented grid cells (i.e. different mountain ranges, where $\Delta f = 1$ and $B > 0$).

The appropriate value of c depends on the importance of topographic facets in the modeling region. In mountainous coastal regions, c is typically set at about 1.5 to 2.0, because of the sharp rain shadows that can occur to the lee of coastal mountains (Table 1). In inland and relatively flat regions, where rain shadows are less pronounced, a value of 1.5 or less will suffice.

The importance of topographic facets in determining climatic patterns varies both spatially and temporally. Therefore, an option can be invoked, if sufficient station data exist, which allows varying amounts of 'crosstalk', or sharing of data points, among topographic facets. Redefining c as the maximum value of the facet weighting exponent, PRISM compares the MAE of the climate-elevation regression line (Eq. 1) from 2 situations: (1) when stations from only the target cell's topographic facet are used; and (2) when all nearby stations are used (constrained by r and s_t). If the addition of stations from other facets increases the MAE by less than a factor of 2, the facet weighting exponent is reduced and the influence of off-facet stations is increased. If the MAE increases by more than this amount, the facet weighting exponent remains unchanged. The factor-of-2 criterion was selected after sensitivity tests suggested that sparse station data often underestimated the true MAE about the regression line by about one-half; therefore, increases in MAE up to twice the original value were not considered to indicate a major shift in climate regime. The new value of c is calculated as follows:

$$C_{new} = c\left(1 - \frac{MAE_a / MAE_b}{0.5}\right);\ 0 \le c_{new} \le c \quad (6)$$

where MAE_a and MAE_b are the mean absolute errors of the elevation regression using stations from the target cell's facet only and with all nearby stations, respectively. Stations entering these regressions are already weighted for distance, elevation, and clustering.

5.3. Olympic Mountains rain shadow

Many coastal mountains produce rain shadows through uplift and blockage of low-level moisture, which enhances precipitation on their windward exposures and reduces precipitation on their leeward sides. The Olympic Mountains in northwestern Washington, containing what are arguably the wettest locations in the continental United States, provide an example. Fig. 2 shows the terrain of the Olympic Peninsula as depicted by a DEM with 500 m grid cell size. At this scale, the Olympic Mountains appear as a series of deeply divided ridges and valleys that together form a roughly elliptical massive. During winter, a nearly continuous series of Pacific frontal systems affects the region. Moisture-bearing winds arriving off the ocean from a generally southwesterly direction are blocked and uplifted by the large-scale bulk of the mountains, producing copious precipitation on the windward slope of the range, but leaving the leeward side in a significant rain shadow. The locations of precipitation stations are shown in Fig. 2. There are few stations in the vicinity of the mountains, especially at higher elevations, making this a challenging area for precipitation mapping.

Fig. 3 shows topographic facet grids for the region at 2 wavelengths, 4 and 60 km. These represent the smallest and largest wavelengths typically used in mapping of precipitation using the PRISM topographic facet weighting functions. Grid cells with the same terrain orientation naturally occur in groups to form contiguous facets. The 4 km wavelength (Fig. 3a), while spatially smoother than the 500 m depiction in Fig. 2, still exhibits small facets made up of few grid cells that are too finely resolved to be physically important for some climatic elements, such as precipitation, and are represented by few stations. The largest-wavelength facets (Fig. 3b) derived from the highly smoothed DEM are very generalized, describing broad scale terrain features and climatically important regimes, such as the windward and leeward slopes of the Olympic Mountains.

Fig. 4a depicts a 1961–1990 mean annual precipitation map for the region. This map was created using

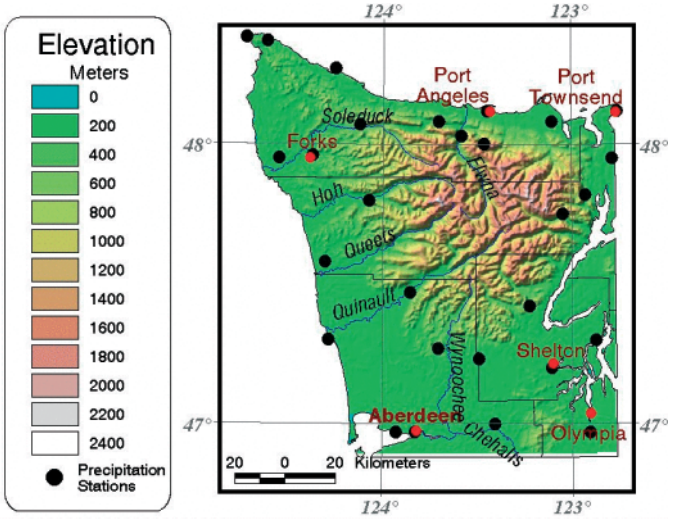

Fig. 2. Terrain map of the Olympic Peninsula, in the northwest corner of Washington State, USA. Terrain resolution is 500 m. Locations of precipitation stations used in mapping are shown as black dots, town locations are red dots

PRISM algorithms that include linear precipitation-elevation regression functions and topographic facet station weighting at each grid cell. The model was run for each month, and the resulting grids summed to produce an annual total. The topographic weighting exponent c was set to 1.8. Strong orographic enhancement of precipitation is clearly evident on the southwestern slopes of the mountains, with annual values exceeding 6000 mm yr^{-1}. In the northeastern portion of the mountains, elevations are relatively high (see Fig. 2), but lack of exposure to the moist southwesterly flow reduces precipitation significantly. Downslope warming and drying along the lower lee slope of mountains produces further drying, culminating in a precipitation minimum of less than 500 mm yr^{-1} on the coastal plain near Port Angeles. The configuration of these precipitation patterns bears a strong similarity to the long-wavelength facet configuration in Fig. 3b. Topographic

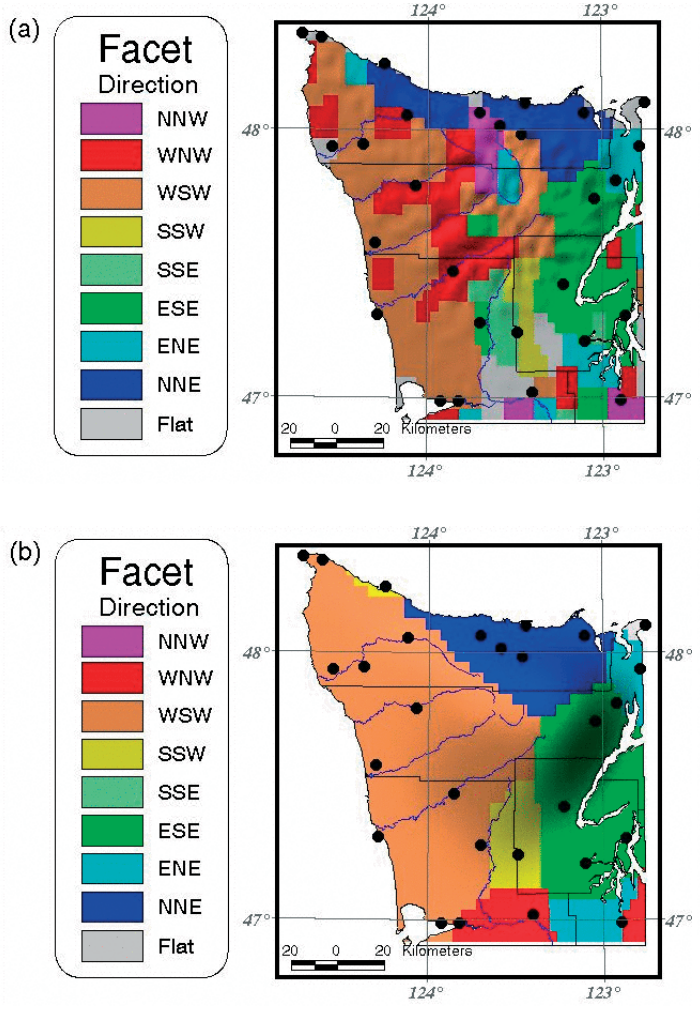

Fig. 3. Topographic facet grids overlain on shaded terrain grids for the Olympic Peninsula delineated at 2 wavelengths: (a) 4 km and (b) 60 km

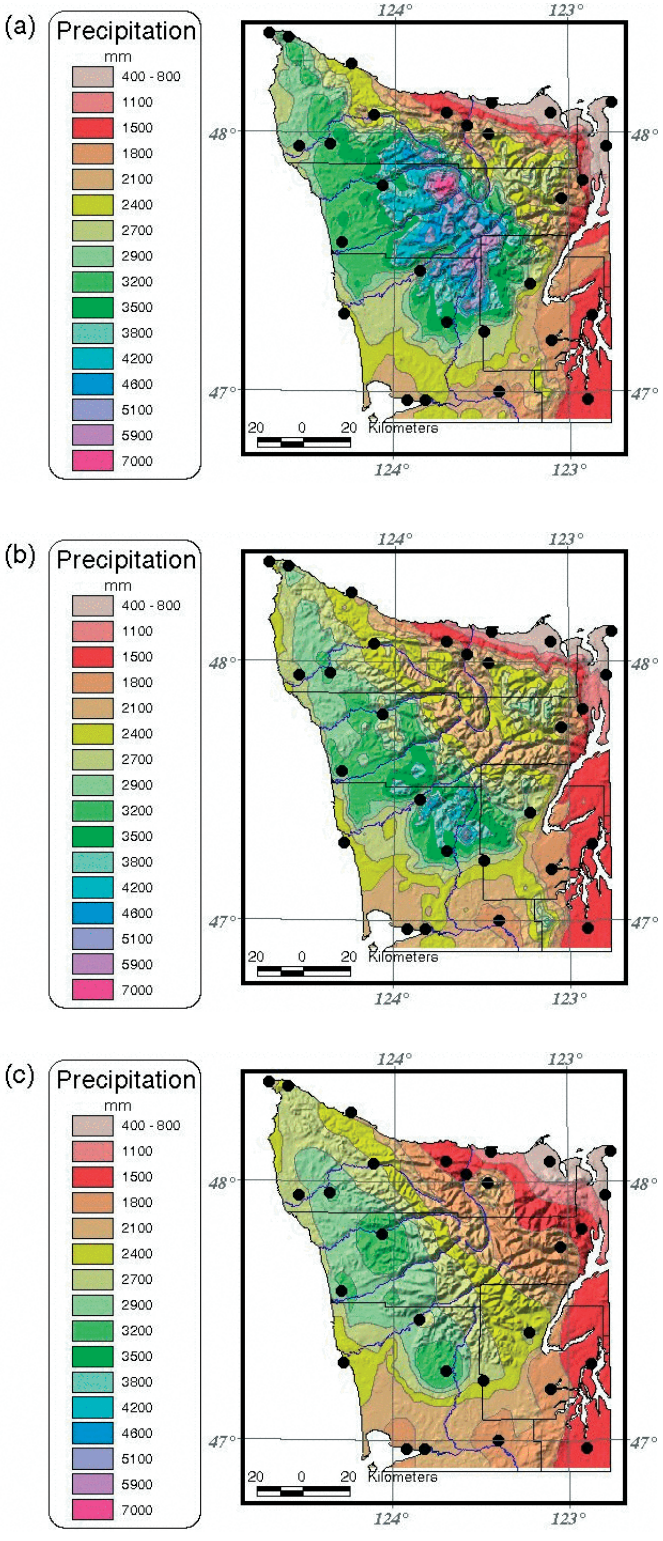

Fig. 4. Mean annual (1961–1990) precipitation overlain on 500 m terrain for the Olympic Peninsula with: (a) elevation regression functions and topographic weighting at each grid cell; (b) same as (a) except without topographic facet weighting; and (c) same as (b) except without terrain (all elevations set to zero). Mapping grid resolution is 4 km

facet weighting effectively constrains the influences of wet (windward) and dry (windward) stations to those areas that are most similar topographically.

Fig. 4b shows a precipitation map produced by the same PRISM algorithms, but with topographic facet weighting turned off ($c = 0$). With nothing to limit the spatial influence of leeward stations, the area of maximum precipitation in the original map (Fig. 4a) 'collapses' to less than 3000 mm yr^{-1}, with only the southern edge remaining intact. Spatial patterns are no longer dictated by the patterns of orographic precipitation dynamics, but rather by the locations and availability of precipitation stations. In Fig. 4c, the effect of elevation is removed altogether by setting all DEM elevations to zero. This essentially leaves nothing but distance as the station weighting function. The resulting map bears little resemblance to the original in Fig. 4a; now, maxima of less than 3500 mm yr^{-1} occur in the vicinity of wetter stations on the windward side of the mountains.

There is independent evidence to suggest that the map in Fig. 4a is closer to the 'true' precipitation field than the others. Modeled precipitation values compare well with runoff from some of the rivers shown in Fig. 2. On the windward side, mean annual runoff is 3452 mm in the Hoh River watershed (1961–1990), 3442 mm in the Queets River watershed (1965–1990), and 4042 mm in the Quinault River watershed (1975–1990) (USDOI-USGS 2001). Estimating that about 30% of the precipitation might be lost to evapotranspiration annually, precipitation on the windward slopes of the Olympics must be at least 4500 to 5000 mm on average, with higher values likely on the upper slopes. The patterns and magnitudes of precipitation in Fig. 4a are also very similar to those of a detailed annual precipitation map for the period 1930-1957 prepared manually by the Soil Conservation Service in 1965, and often referred to as the 'official' precipitation map of Washington (USDA-SCS 1965). The area of maximum precipitation on this map is in exactly the same location as in Fig. 4a, and exceeds 6100 mm, compared to 7000 mm in Fig. 4a.

6. COASTAL PROXIMITY

Coastal proximity grids have been developed that estimate the proximity of each grid cell to major water bodies. These grids are derived from a variety of sources that vary from a simple measure of distance from a coastline in relatively flat terrain, to outputs from algorithms that model the penetration of marine influence into complex terrain. This information is used to select and weight stations according to their similarity in coastal proximity to the target grid cell.

6.1. Calculation of the coastal proximity weight

The coastal proximity weight for a station is calculated as:

$$W(p) = \begin{Bmatrix} 1;\ \Delta p = 0 \\ 0;\ \Delta p > p_x \\ \dfrac{1}{\Delta p^v};\ 0 < \Delta p \le p_x \end{Bmatrix} \quad (7)$$

where Δp is the absolute difference between the station and target grid cell coastal proximity index, v is the coastal proximity weighting exponent, and p_x is the maximum proximity difference. The exponent v is typically set at 1.0 for regions where coastal effects are significant (Table 1). If Δp for a station exceeds p_x, that station's weight becomes zero (Table 1).

6.2. Coastal California temperature gradient

The usefulness of coastal proximity weighting is exemplified when mapping August maximum temperature along the central California coast. During summer, marine upwelling in an already cool offshore current, in combination with northwesterly (onshore) winds, keeps the coastal strip much cooler than areas just a few kilometers inland. This effect is relatively continuous up and down the coastline, with occasional penetration of coastal air into inland valleys exposed to the ocean. The coastal/inland temperature gradient is greatest where inland penetration is blocked by mountains near the coastline. Unfortunately, the distribution of coastal and inland temperature stations has significant gaps, and it does not always depict the situation accurately (Fig. 5).

Without coastal proximity weighting, the PRISM-predicted mean August maximum temperature map exhibited tongues of warm temperature, influenced by inland observations, interrupting the coastal temperature field where there are no coastal stations (e.g. Point Reyes, northwest of San Francisco; Fig. 5a). Conversely, a lack of inland stations allowed too much coastal influence in areas where terrain blockage of marine penetration was known to be significant (e.g. Big Sur area, south of Monterey, Fig. 5a).

An advection algorithm that simulates the penetration of marine influence into complex terrain was used to generate a coastal proximity grid for PRISM, and coastal proximity weighting was applied (z = 1.0). The result was a significant reduction in the influence of inland stations on coastal temperature estimation, and vice versa. A relatively continuous,

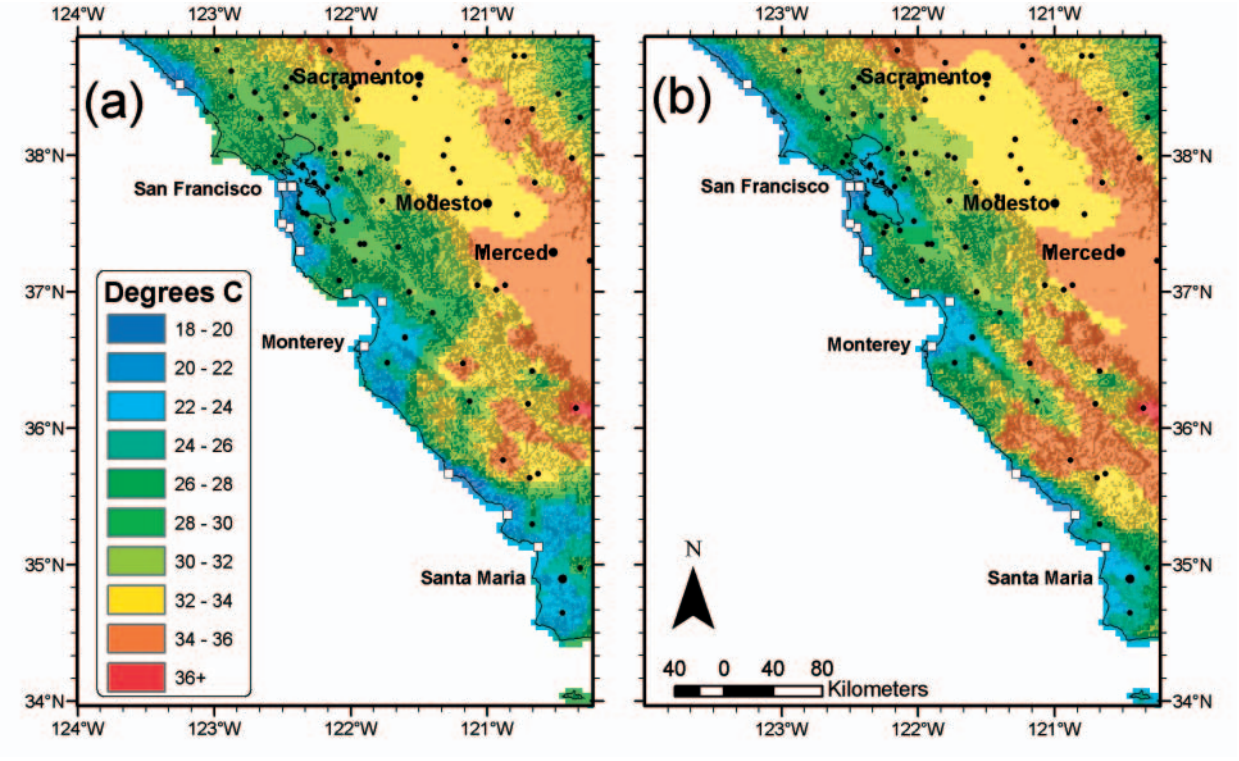

Fig. 5. Map of 1961–1990 mean August maximum temperature for the coast of central California (a) without and (b) with coastal proximity weighting. Open squares denote locations of coastal stations. Solid dots denote inland stations. Modeling grid resolution is 4 km

and more realistic, strip of cooler temperatures along the coast was simulated, with limited areas of penetration inland (e.g. Salinas Valley, southeast of Monterey; Fig. 5b). Jackknife cross-validation errors helped quantify the effectiveness of coastal proximity weighting. Without proximity weighting, the MAE for the 12 coastal stations shown in Fig. 5 was 5.0°C. With proximity weighting, the MAE was reduced to 1.6ºC.

7. THE TWO-LAYER ATMOSPHERE

To simulate situations where non-monotonic relationships between climate and elevation are possible (e.g. temperature inversions and mid-slope precipitation maxima), climate stations entering the regression are divided into 2 vertical layers. Layer 1 represents the boundary layer and layer 2 the free atmosphere above it. Stations in the same layer as the target grid cell receive full weight, while those in the adjacent layer receive lower weights. In essence, the layer weighting scheme limits the ability of stations in one layer to influence the regression function of the other.

7.1. Calculation of the vertical layer weight

The vertical layer weight for a station is calculated as:

$$W(l) = \left\{ \begin{array}{l} 1;\ \Delta l = 0 \text{ or } \Delta z \le \Delta z_m \\ \dfrac{1}{(\Delta z - \Delta z_m)^y};\ \Delta l = 1 \text{ and } \Delta z > \Delta z_m \end{array} \right\} \quad (8)$$

where Δl is the absolute layer difference between the station and the target grid cell (1 for adjacent layer, 0 for same layer), Δz is the absolute elevation difference between the station and the target grid cell, and y is the vertical layer weighting exponent. If the station and target grid cell are in the same layer, the layer weight is 1. If not, the layer weight depends on their elevation difference. As in elevation weighting, the elevation difference is subject to Δz_m, the minimum elevation difference. If the elevation difference between the station and the target grid cell is less than Δz_m, even if station and cell are in different layers, the layer weight is 1. As a result, the boundary between layers 1 and 2 is 'fuzzy', with a region around this boundary that shares stations from both layers. The

appropriate value of y depends on the importance of a boundary layer or inversion in the modeling region. A value of 0.5 to 1.0 is often used where trade-wind inversions or cold-air drainage are expected to produce reversals in the lapse of rainfall or temperature (Table 1).

When the crosstalk option is invoked, PRISM calculates the spatially and temporally varying strength of inversions and boundary layer integrity in the same manner as is used for topographic facets (see Eq. 6). Redefining y as the maximum value of the layer weighting exponent, PRISM compares the MAE of the climate-elevation regression line (Eq. 1) from 2 situations: (1) when stations from only the target cell's layer are used, and (2) when all nearby stations are used (constrained by r and s_t). If the addition of stations from the adjacent vertical layer increases the MAE by less than a factor of 2 (see Section 5.2 for explanation), the layer weighting exponent is reduced (Eq. 6) and crosstalk is thereby increased. If the MAE increases by more than this amount, the layer weighting exponent remains unchanged.

7.2. Estimation of potential wintertime inversion height

A simple method was developed to spatially distribute the height of the top of the wintertime inversion layer, should it exist, for use in mapping temperature. While this method may be overly simplistic for some uses, in this case it is not necessary that the estimated height be extremely accurate, because it is subject to Δz_m, which varies from about 100 to 300 m. In addition, the inversion height represents only a candidate dividing line between stations, which may be partially or fully dissolved if the relationship between the climate element and elevation is similar above and below it. Use of the potential inversion height grid in PRISM modeling is restricted to regions and seasons for which temperature inversions are known to exist.

A grid of elevations representing the top of the boundary layer for the contiguous United States under wintertime temperature inversions was prepared using a 2.5 min DEM by: (1) finding the minimum elevation of all grid cells within an approximately 40 km radius of each grid cell of interest; (2) low-pass filtering this minimum elevation grid by averaging all cells within a 40 km radius to produce a smooth, 'base' elevation grid; and (3) adding a constant, climatological inversion height to the base elevations. After performing sensitivity tests, 40 km was subjectively chosen as the search and averaging radius, because this scale was small enough to discern many small mountain/valley systems, but large enough to give a stable field that avoided including very small-scale features that were best represented as parts of larger scale mountain/valley systems. Radii other than 40 km may be appropriate for modeling domains of different size and resolution than the contiguous United States at 2.5 min, but insufficient information has been gathered to generalize the procedure.

Analyses of radiosonde data from several cities in the United States with persistent, climatological inversions indicated that the inversion top typically occurred at 200 to 300 m above ground level. The inversion top was quite consistent; when an inversion formed, it tended to do so at about the same height each time. Therefore, 250 m was added to the base elevation at each grid cell to obtain the potential inversion height above sea level. A potential wintertime inversion height grid for the contiguous United States is shown in Fig. 6. Valleys and other depressions tend to fall within the boundary layer, while local ridge tops and other elevated terrain emerge into the free atmosphere (Johnson et al. 2000).

8. SUMMARY AND CONCLUSIONS

For the most of the 20th century, climate maps were produced manually by expert climatologists using pen and paper. These maps were considered the best available, but were rarely updated because of the large amount of effort and expense involved in their production. Beginning in the latter part of the 20th century and continuing today, the demand for updated, GIS-compatible climate maps has increased dramatically. In response, a variety of computerized statistical techniques have been used to facilitate the production of such maps. However, observational data are often too sparse and unrepresentative to enable statistical

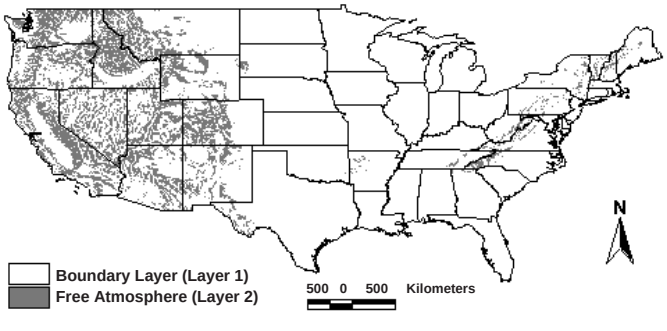

Fig. 6. Estimated wintertime inversion layer grid for the conterminous US. Shaded areas denote terrain estimated to be in the free atmosphere (layer 2) under winter inversion conditions, should they develop. Unshaded areas are expected to be within the boundary layer (layer 1). Grid resolution is 4 km

approaches to directly create high-quality climate maps that truly represent the state of knowledge. While these approaches have a great potential advantage over human-expert methods in terms of speed, consistency, and repeatability, they lack a spatial climate knowledge base that can be drawn upon to fill the need for expertise and experience in the mapping process.

An effective hybrid approach is to use the wealth of knowledge on climate mapping to help enhance, control, and parameterize a statistical technique. To that end, the objective of this paper was to describe the thinking and rationale behind the development of a spatial climate knowledge-based system (KBS) and to present working examples in the form of algorithms from a statistical regression model known as PRISM (parameter-elevation regressions on independent slopes model). The ultimate goal is to develop an expert system capable of reproducing the process a knowledgeable climatologist would use to create high-quality climate maps, with the added benefits of consistency and repeatability. However, knowledge must first be accumulated and evaluated through an ongoing process of model application; development of knowledge prototypes, parameters, and parameter settings; testing; evaluation; and modification.

The knowledge base presented here draws upon over a century of observations and research in a discipline that can be termed 'geospatial climatology', the study of the spatial patterns of climate and their relationships with geographic features. The basic concept is the strong variation of climate with elevation. Elevation is an excellent statistical predictor variable, because it is usually sampled at a far greater spatial density than climate variables and is often estimated on a regular grid. This climate-elevation relationship takes the statistical form of a weighted climate-elevation regression function. The regression function is evaluated independently at each grid cell, in a moving-window fashion, to account for spatial variations in the climate-elevation relationship. Climate stations are assigned weights that account for other climatically important factors besides elevation. Aspect and topographic exposure, which affect climate at a variety of scales, from hill slope to windward and leeward sides of mountain ranges, are simulated by dividing the terrain into topographic facets. A coastal proximity measure is used to account for sharp climatic gradients near coastlines. A 2-layer model structure divides the atmosphere into a lower boundary layer and an upper free atmosphere layer, allowing the simulation of temperature inversions, as well as mid-slope precipitation maxima. The effectiveness of various terrain configurations at producing orographic precipitation enhancement is also estimated.

While ongoing development will undoubtedly result in the continued addition of knowledge concerning the relationships between climate and geographic variables, effort is also focused on providing dynamically based knowledge to the system. For example, a trajectory module that calculates relative moisture loss over terrain barriers during mean onshore storm flow has been developed and used in precipitation modeling applications in Alaska and British Columbia, where data were too sparse to properly locate many significant rain shadows. A second model that simulates the penetration of a shallow marine layer onshore into complex terrain has been used for coastal temperature mapping along the west coast of the USA and Canada (e.g. see Section 6.2).

Both the knowledge base and resulting PRISM algorithms are in a state of constant development. Current information on mapping activities and access to a large selection of digital climate layers are available on the World Wide Web at http://www.ocs.orst.edu/prism/ and http://www.climatesource.com.

Acknowledgements. PRISM model and product development has been supported in part by the USDA Natural Resource Conservation Service, National Water and Climate Center; NOAA Office of Global Programs, NOAA National Climatic Data Center, NOAA Western Regional Climate Center; USDA Forest Service; and NOAA National Weather Service. We thank M. Doggett and T. Parzybok for preparing the figures.

LITERATURE CITED

Barnes SL (1964) A technique for maximizing details in numerical weather map analysis. J Appl Meteorol 3:396–409

Barry RG, Chorley RJ (1987) Atmosphere, weather and climate, 5th edn. Routledge, London

Basist A, Bell GD, Meentemeyer V (1994) Statistical relationships between topography and precipitation patterns. J Clim 7:1305–1315

Bishop GD, Church MR, Daly C (1998) Effects of improved precipitation estimates on automated runoff mapping: eastern United States. J Am Water Resour Assoc 34:159–166

Bootsma A (1976) Estimating minimum temperature and climatological freeze risk in hilly terrain. Agric For Meteorol 16:425–443

Burns JI (1953) Small-scale topographic effects on precipitation distribution in San Dimas Experimental Forest. Trans Am Geophys Union 34:761–768

Daly C (2002) Variable influence of terrain on precipitation patterns:delineation and use of effective terrain height in PRISM. Oregon State University, Corvallis; available at http://www.ocs.orst.edu/prism/effter.pdf

Daly C, Johnson GL (1999) PRISM spatial climate layers: their development and use. Short course on topics in applied climatology, 79th Ann Meeting Am Meteorol Soc, 10–15 January, Dallas, TX. American Meteorological Society; available at http://www.ocs.orst.edu/prism/prisguid.pdf

Daly C, Neilson RP (1992) A digitial topographic approach to modeling the distribution of precipitation in mountainous

terrain. In: Jones ME, Laenen A (eds) Interdisciplinary approaches in hydrology and hydrogeology. American Institute of Hydrology, Minneapolis, p 437–454
Daly C, Neilson RP, Phillips DL (1994) A statistical-topographic model for mapping climatological precipitation over mountainous terrain. J Appl Meteorol 33:140–158
Daly C, Taylor GH, Gibson WP (1997) The PRISM approach to mapping precipitation and temperature. In: Proc 10th AMS Conf Appl Climatol, Reno, NV, October 20–23. American Meteorological Society, p 10–12
Daly C, Kittel TGF, McNab A, Royle JA and 5 others (1999) Development of a 102-year high-resolution climate data set for the conterminous United States. In: Proc 10th Symposium on Global Change Studies, 79th Annual Meeting of the American Meteorological Society, 10–15 January, Dallas TX, 480–483
Daly C, Gibson WP, Hannaway D, Taylor GH (2000a) Development of new climate and plant adaptation maps for China. In: Proc 12th AMS Conf Appl Climatol, Asheville, NC, May 8-11. American Meteorological Society, p 62–65
Daly C, Kittel TGF, McNab A, Gibson WP, Royle JA, Nychka D, Parzybok T, Rosenbloom N, Taylor GH (2000b) Development of a 103-year high-resolution climate data set for the conterminous United States. In: Proc 12th AMS Conf Appl Climatol, Asheville, NC, May 8–11. American Meteorological Society, p 249–252
Daly C, Taylor GH, Gibson WP, Parzybok TW, Johnson GL, Pasteris P (2001) High-quality spatial climate data sets for the United States and beyond. Trans Am Soc Agric Eng 43:1957–1962
Dingman SL, Seely-Reynolds DM, Reynolds RC III (1988) Application of kriging to estimate mean annual precipitation in a region of orographic influence. Wat Resour Bull 24:29–339
Dodson R, Marks D (1997) Daily air temperature interpolated at high spatial resolution over a large mountainous region. Clim Res 8:1–20
Doukidis GI, Whitley EA (1988) Developing expert systems. Chartwell-Bratt, Lund
Environment Canada (2001) Southern British Columbia climate change impacts resources: maps and scenarios. available at http://www.pyr.ec.gc.ca/climate-change/index_e.htm
Forsyth R (1989) The expert system phenomenon. In: Forsyth R (ed) Expert systems: principles and case studies. Chapman & Hall, London
Garen DC, Johnson GL, Hanson CL (1994) Mean areal precipitation for daily hydrologic modeling in mountainous terrain. Wat Resour Bull 30:481–491
Giambelluca TW, Nullet D (1991) Influence of the trade-wind inversion on the climate of a leeward mountain slope in Hawaii. Clim Res 1:207–216
Gibson WP, Daly C, Taylor GH (1997) Derivation of facet grids for use with the PRISM model. In: Proc 10th AMS Conf Appl Climatol, Reno, NV, October 20–23. American Meteorological Society, p 208–209
Hanson CL (1982) Distribution and stochastic generation of annual and monthly precipitation on a mountainous watershed in southwest Idaho. Wat Resour Bul 18:875–883
Hevesi JA, Istok JD, Flint AL (1992) Precipitation estimation in mountainous terrain using multivariate geostatistics. 1. Structural analysis. J Appl Meteorol 31:661–676
Hibbert AR (1977) Distribution of precipitation on rugged terrain in central Arizona. Hydrol Water Resour Ariz Southwest 7:163–173
Holt A, Benwell GL (1999) Applying case-based reasoning techniques in GIS. Int J Geog Info Sci 13:9–25
Houghton JG (1979) A model for orographic precipitation in the north central Great Basin. Mon Weather Rev 107: 1462–1475
Hovecar A, Martsolf JD (1971) Temperature distribution under radiation frost conditions in a central Pennsylvania valley. Agric Meteorol 8:371–383
Hutchinson MF (1995) Interpolating mean rainfall using thin plate smoothing splines. Int J GIS 9:385–403
Johnson GL, Daly C, Hanson CL, Lu YY, Taylor GH (2000) Spatial variability and interpolation of stochastic weather simulation model parameters. J Appl Meteorol 39(6): 778–796
Jones EK, Roydhouse A (1994) Intelligent retrieval of historical meteorological data. AI Appl 8(3):43–54
Juvik JO, Nullet D, Banko P, Hughes K (1993) Forest climatology near the tree line in Hawai'i. Agric For Meteorol 66:159–172
Lam DCL, Swayne DA (1993) An expert system approach of integrating hydrological database, models and GIS: application of the RAISON System. In: Kovar K, Nachtnebel HP (eds) Proc Appl GIS Hydrol Wat Resour Manag, Vienna, April 1993. Publ. No. 211, International Association of Hydrological Sciences, Wallingford, p 23–34
Matheron G (1971) The theory of regionalized variables and its applications. Cahiers du Centre de Morphologie Mathematique, Ecole des Mines, Fountainebleau
Neilson RP (1995) A model for predicting continental-scale vegetation distribution and water balance. Ecol Appl 5:362–385
Nemani R, Running SW, Band LE, Peterson DL (1993) Regional hydroecological simulation system: an illustration of the integration of ecosystem models in a GIS. In: Goodchild MF, Parks BO, Steyaert LT (eds) Environmental modeling with GIS. Oxford University Press, New York, p 296–304
Nusser SM, Goebel JJ (1997) The national resources inventory: a long-term multi-resource monitoring programme. Environ Ecol Stat 4(3):181–204
Oke TR (1978) Boundary layer climates. Methuen, London
Osborn HB (1984) Estimating precipitation in mountainous regions. J Hydraul Eng 110:1859–1863
Peck EL, Brown MJ (1962) An approach to the development of isohyetal maps for mountainous areas. J Geophys Res 67:681-694
Phillips DL, Dolph J, Marks D (1992) A comparison of geostatistical procedures for spatial analysis of precipitation in mountainous terrain. Agric For Meteorol 58:119–141
Plantico MS, Goss LA, Daly C, Taylor GH (2000) A new US climate atlas. In: Proc 12th AMS Conf Appl Climatol, Asheville, NC, May 8–11. American Meteorological Society, p 247–248
Reed WG, Kincer JB (1917) The preparation of precipitation charts. Mon Weather Rev 45:233–235
Renka RJ (1984) Interpolation of data on the surface of a sphere. ACM Trans Math Soft 10:417–436
Schermerhorn VP (1967) Relations between topography and annual precipitation in western Oregon and Washington. Wat Resour Res 3:707–711
Schmoldt DL, Rauscher HM (1996) Building knowledge-based systems for natural resource management. Chapman & Hall, New York
Schwarb M, Daly C, Frei C, Schar C (2001a) Mean seasonal precipitation throughout the European Alps, 1971-1990. Hydrologic Atlas of Switzerland, National Hydrologic Service, Bern
Schwarb M, Daly C, Frei C, Schar C (2001b) Mean annual precipitation throughout the European Alps, 1971–1990.

Hydrologic Atlas of Switzerland, National Hydrologic Service, Bern
Shepard D (1968) A two-dimensional interpolation function for irregularly spaced data. In: Proc 23rd National Conf ACM. American Meteorological Society, p 517–523
Spreen WC (1947) A determination of the effect of topography upon precipitation. Trans Am Geophys Union 28:285–290
Stoeckeler JH (1963) Springtime frost frequency near LaCrosse, Wisconsin, as affected by topographic position, and its relation to reforestation problems. J For 61: 379–381
Studer R, Fensel D, Decker S, Benjamins VR (1999) Knowledge engineering: survey and future directions. In: Puppe F (ed) XPS-99: knowledge-based systems, survey and future and directions. 5th Biann German Conf Knowledge-Based Syst, Wurzburg, Germany, March 1999. Lecture Notes in Artificial Intelligence 1570. Springer, Berlin, p 1–23
Thornton PE, Running SW, White MA (1997) Generating surfaces of daily meteorological variables over large regions of complex terrain. J Hydrol 190:214–251
USDA-NRCS (1998) PRISM Climate Mapping Project - precipitation. Mean monthly and annual precipitation digital files for the continental US. CD-ROM, USDA Natural Resources Conservation Service, National Cartography and Geospatial Center, Ft. Worth, TX
USDA-SCS (1965) Mean Annual Precipitation 1930–1957, State of Washington. Weather Bureau River Forecast Center, Portland, OR. USDA Soil Conservation Service, Washington, DC
USDOC (1968) Climatic atlas of the United States. Environmental Data Service, Environmental Science Services Administration, US Department of Commerce, Washington, DC
USDOI-USGS (2001) Calendar year streamflow statistics for Washington. Water Resources of Washington, US Geologic Survey, Boulder, CO; available at http://water.usgs.gov/wa/nwis/annual
Vogel RM, Wilson I, Daly C (1999) Regional regression models of annual streamflow for the United States. J Irrig Drainage Eng 125:148–157
Vuglinski VS (1972) Methods for the study of laws for the distribution of precipitation in medium-high mountains (illustrated by the Vitim River Basin). Distribution of precipitation in mountainous areas, WMO Publ 326(2):212–221
Wahba G, Wendelberger J (1980) Some new mathematical methods for variational objective analysis splines and cross validation. Mon Weather Rev 108:1122–1143

Editorial responsibility: Robert Davis, Charlottesville, Virginia, USA

Submitted: October 1, 2001; Accepted: January 17, 2002
Proofs received from author(s): July 17, 2002